Application of the adjacency matrix eigenvectors method to geometry determination of toroidal carbon molecules

Ante Graovac, Dejan Plavšić, Matjaž Kaufman, Tomaž Pisanski, and Edward C. Kirby

Citation: The Journal of Chemical Physics **113**, 1925 (2000); doi: 10.1063/1.481996
View online: http://dx.doi.org/10.1063/1.481996
View Table of Contents: http://scitation.aip.org/content/aip/journal/jcp/113/5?ver=pdfcov
Published by the AIP Publishing

Application of the adjacency matrix eigenvectors method to geometry determination of toroidal carbon molecules

Ante Graovac[a] and Dejan Plavšić
The Rudjer Bošković Institute, HR-10002 Zagreb, POB 180, Croatia

Matjaž Kaufman and Tomaž Pisanski
Institute for Mathematics, Physics and Mechanics, Jadranska 19, SI-1000 Ljubljana, Slovenia

Edward C. Kirby
Resource Use Institute, Pitlochry, Perthshire PH16 5DS, Scotland, United Kingdom

(Received 6 July 1999; accepted 2 May 2000)

Torusenes are defined as closed toroidal networks where every vertex or atom is 3-valent, and they can represent pure carbon tori. Here we study the geometries of two classes: hexagonal torusenes containing purely polyhex networks and the second class, 5,6,7-ring torusenes which besides hexagons contain also an equal number of 5- and 7-membered rings. As sophisticated quantum-mechanical methods for geometry determination are time consuming for large carbon cages, and having in mind the huge number of their isomers, one is interested in methods which are simple to apply but which are still able to produce plausible geometries. One of them is offered by the adjacency matrix elgenvectors (AME) method, which was proposed in this journal [D. E. Manolopoulos and P. W. Fowler, J. Chem. Phys. **96**, 7603 (1992)]. The application of the AME method to fullerenes is based on an appropriately chosen triplet of eigenvectors. A rational choice may be made on the basis of their nodal properties. No rules have been formulated up to now on how to apply the AME method to torusenes. In order to find such a rule a systematic study of nodal properties of torusenes is crucial, and such a study is the subject of this paper. Theoretical and computer experimental considerations presented here suggest that a triplet $\mathbf{a}_2, \mathbf{a}_3, \mathbf{a}_{\text{opt}}$ fulfills the task where the $\mathbf{a}_{\text{opt}}$ should be checked for among those eigenvectors which possess no radial nodal plane but have one axial cut. In the present paper these findings have been elaborated for 5,6,7-ring torusenes with up to 270 atoms, and computer experiments have shown that similar findings hold for purely polyhex torusenes with up to 224 carbon atoms as well. In order to understand better these nodal properties, a quantum-mechanical study of free electrons on the surface of a torus was also undertaken. © *2000 American Institute of Physics.* [S0021-9606(00)00829-1]

I. INTRODUCTION

Fullerenes, carbon nanotubes, and torusenes have become a subject of intensive research (see, for example, Ref. 1). As the number of possible isomers of such pure carbon cages grows very fast as the number of carbon atoms increases,[2] it is highly desirable, after generating (all of) them[3] to sort out the most stable ones. A series of rules have been developed to do such a sorting, with the isolated-pentagon (IP) rule[4,5] having a prominent role. However, by applying the IP and supplementary rules to a carbon cage, one is still faced with a huge number of feasible isomers. The determination of geometry of carbon cages could be addressed by means of sophisticated methods of electronic structure calculations, molecular mechanics or molecular dynamics computations. However, as all these procedures are time consuming when applied to large carbon cages and having in mind the huge number of their isomers, it is worthwhile to search for methods of structure determination of carbon cages which are simple to apply but which are still able to produce plausible geometries.

The adjacency matrix eigenvectors (AME) method is one of the most popular for obtaining a plausible geometric representation of fullerenes and other spheroidal cages.[6–9] As torusenes (sp^2-hybridized pure carbon structures in the shape of a torus) have now probably been experimentally detected[10] as well as studied theoretically,[11] it is worthwhile to see whether the AME is able to reproduce geometries of these novel structures. For general graphs the Laplacean matrix eigenvector (LME) method gives better results than the AME method. However, as here we consider 3-valent pure carbon cages, i.e., the regular graphs with valency 3, the LME drawings do not differ from the AME ones.

The application of the AME to fullerenes is based on an appropriate choice of a triplet of eigenvectors, and the eigenvectors associated with eigenvalues 2, 3, and 4, which often is a good choice for conventional (graph-theoretically planar) fullerenes,[7] does not generally work well for toroidal species. The choice is governed by the nodal properties of eigenvectors. No rules have been formulated up to now for torusenes,

[a]Also at Faculty of Natural Sciences, Mathematics and Education, University of Split, Nikole Tesle 12, HR-21000 Split, Croatia.

although a few ad hoc results have appeared.[12,13] For any systematic study of torusenes a knowledge of their nodal properties is crucial. Such a study is presented here, and is performed within the AME method. However, in order to illuminate nodal properties of torusenes, a simple model of free electrons on the surface of a torus is studied first in the next section. If we start with a qualitative picture, we can assume that the eigenvalues used to order the eigenvectors measure a wave energy, and this roughly increases with the length of the nodal boundary. The first two useful eigenvectors ($\mathbf{a}_2$ and $\mathbf{a}_3$) may be thought of as identifying planes containing the symmetry axis of the torus, while the last eigenvector, if it is to be useful, will contain a single nodal cut, orthogonal to the symmetry axis. Since this cut has greater length, and consequent higher energy (especially for large diameter thin-tubed tori, where R/r is large), this eigenvector is likely to be found further along the eigenvalue-ordered sequence.

The eigenvectors of a torus have been studied also in Ref. 14, where hexagonal coverings on the torus and Klein bottle have been enumerated (a computer algorithm for enumerating the former was described in Ref. 15). Kekulé structures of torusenes are discussed in Ref. 16.

II. QUANTUM-MECHANICAL CONSIDERATIONS

Consider first a relevant closed surface before any embedding of a carbon network has taken place. For example, it is the surface of a sphere for fullerenes and that of a torus for torusenes. A good starting point, and a reasonable approximation, is to treat n π-electrons, of a carbon cage with n carbon atoms, as being simply an ensemble of n free electrons on the given surface. In this case, instead of eigenvectors, we speak about electronic wave functions. The nodal properties of eigenvectors can be then deduced from nodal properties of these wave functions. The quantum-mechanical (QM) solution for the electrons on a unit sphere is well known, with wave functions being given by

$$\Psi_{l,m}(\vartheta,\varphi)=P_{l,m}(\cos\vartheta)e^{im\varphi}, \tag{1}$$

where and ϑ and φ are spherical angle coordinates (defined in the standard way with respect to x-, y-, and z-axes), and $\Psi_{l,m}$ are usual spherical harmonics with $l=0,1,2,...$, and $m=-l,-l+1,...+l$. The angular momentum quantum number l equals the number of nodal planes parallel to the xy-plane, and the magnetic quantum number m equals the number of nodal planes passing through the z-axis. The angle between these planes is $2\pi/m$ (for $m=0$ there is no such plane), while the distance between planes parallel to the xy-plane is determined by zeros of the Legendre polynomial part, $P_{l,m}$, of the spherical harmonic. The nodal properties of free electrons on a sphere are of use in interpreting the nodal properties of the adjacency matrix eigenvectors of fullerenes. Therefore, we proceed to surfaces appropriate to describe torusenes.

The QM wave functions for free electrons on the surface of the cylinder with radius r (depicted in Fig. 1) are also well known and are given by

$$\Psi_{m,\mu}(\varphi,\mu)=e^{im\varphi}e^{i\mu z}, \tag{2}$$

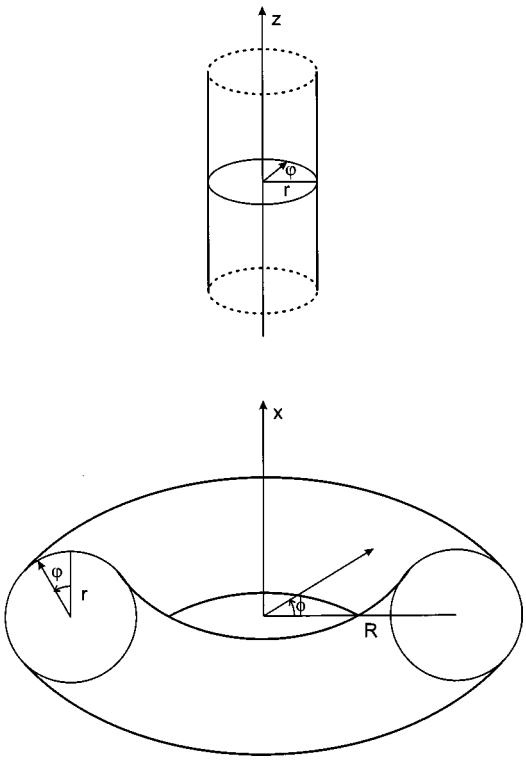

FIG. 1. Definitions of coordinates for cylinder and torus.

where m is again the integer $m=\ldots,-1,0,1,...$, but μ is any real number for an infinite cylinder. The quantum number m defines the number of nodal planes passing through the z-axis. We call them *axial nodal planes*. These nodal planes are better visualized if each pair of *degenerate* functions $e^{im\varphi}$ and $e^{-im\varphi}$ is substituted by a pair of their real counterparts, $\cos m\varphi$ and $\sin m\varphi$, where now, $m=0,1,2,...$. The number m now equals the number of axial nodal planes. The quantum number μ becomes an integer $M=\ldots,-1,0,1,...$ when one closes the cylinder on itself to form a torus, as depicted in Fig. 1.

Instead of the coordinate z, the second angle Φ appears, and the QM wave functions for the free electrons on the surface of the torus can be written as

$$\Psi_{m,M}(\varphi,\Phi)=e^{im\varphi}e^{iM\Phi}, \tag{3}$$

where $m=\ldots,-1,0,1,...$ and $M=\ldots,-1,0,1,...$. The quantum number M defines the number of nodal planes passing through the x-axis (torus axis perpendicular to the torus plane). We call them *radial nodal planes*. They are better visualized if each pair of degenerate functions $e^{iM\Phi}$ and $e^{-iM\Phi}$ is substituted by a pair of their real counterparts $\cos M\Phi$ and $\sin M\Phi$. In such a way the QM wave functions could be rewritten in their real form as

$$\Psi^{\text{real}}_{m,M}(\varphi,\Phi)\begin{cases}\cos m\varphi\cdot\cos M\Phi\\ \sin m\varphi\cdot\cos M\Phi\\ \cos m\varphi\cdot\sin M\Phi\\ \sin m\varphi\cdot\sin M\Phi\end{cases}, \tag{4}$$

where $m=0,1,2,...$ and $M=0,1,2,...$.

The above functions obviously are equivalent to the following quartet (of pairwise degenerate) complex wave functions: $\Psi_{m,M}$, $\Psi_{-m,M}$, $\Psi_{m,-M}$, $\Psi_{-m,-M}$. The number M equals the number of *radial* planes, and the number m equals the number of surfaces which cut the torus all round and in an analogy with the cylinder we call them *axial cuts*.

For a torus with given radii r and R, the dependence of energies of free electrons on quantum numbers m and M is easy to obtain. The ordering of energies, but not the nodal properties, is changed when one goes from the free-electron model to some other more realistic one. The model we use later on is based on the first neighbor interactions of π-electron centers in carbon cages, i.e., on the adjacency matrix model of a graph representing the cage. Accordingly, instead of nodal properties of wavefunctions we talk of nodal properties of the adjacency matrix eigenvectors.

III. METHOD

The AME algorithm,[6–8] being already in use by some fullerene research groups, is based on consideration of the eigenvectors $\mathbf{a}_1,\mathbf{a}_2,\ldots,\mathbf{a}_n$ of the adjacency matrix $\mathbf{A}$ of a graph $\mathbf{G}$ with n vertices. The eigenvalues of $\mathbf{A}$ are ordered as $\lambda_1>\lambda_2>\cdots$. The triplet of eigenvectors $\mathbf{a}_j,\mathbf{a}_k,\mathbf{a}_l$ is taken to build an $n\times 3$ matrix $\mathbf{B}=[\mathbf{a}_j,\mathbf{a}_k,\mathbf{a}_l]$. By reading the ith row of $\mathbf{B}$, $[a_{ij}\,a_{ik}\,a_{ij}]$, as the three-dimensional (3D) coordinates of vertex i, and running over all i values, a 3D-drawing of $\mathbf{G}$ is achieved. For general graphs the Laplacean matrix eigenvector (LME) method gives better results than the AME method. However, as here we consider σ 3-valent pure carbon cages, i.e., regular graphs of degree 3, the LME drawings are the same as the AME ones.

The question then arises as to how to choose the triplet of eigenvectors to obtain the most realistic geometry. In the case of regular graphs, the eigenvector $\mathbf{a}_1$ consists of all-ones; $\mathbf{a}_1=(1,1,...,1)^t$ and is of little use, since the drawing is then necessarily in the plane spanned by the other two coordinates. In the papers[6–8] the argument favors the triplet of consecutive eigenvectors, $\mathbf{a}_2,\mathbf{a}_3,\mathbf{a}_4$, to produce plausible 3D-representations of fullerenes. However, a few counterexamples are cited in the literature.[6]

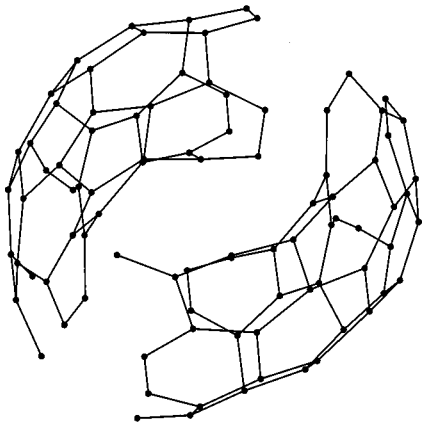

FIG. 3. A drawing (produced by the spring embedder method) of two radial-nodal fragments for the third adjacency-matrix eigenvector of the 5-6-7-ring torusene T_1, with six 5- and six 7-membered rings, having 90 vertices, is shown.

The aim of the present paper is to formulate a rule for which triplet of eigenvectors one should choose to obtain realistic geometries of torusenes. Therefore, we first present a study of the nodal properties of a few selected torusenes.

For visualizing nodal properties of each eigenvector $\mathbf{a}_j=(a_{1j},a_{2j},\ldots,a_{nj})t$ we use the following technique, derived from the one described in Refs. 6 and 17. We assign to each vertex i the corresponding coefficient a_{ij} of its jth eigenvector $\mathbf{a}_j$. Then we construct a subgraph of $\mathbf{G}$ containing all vertices of $\mathbf{G}$ but only those edges that have the same sign of coefficients on both their endpoints. We call such a graph a *fragmented* graph (of the jth eigenvector), and it contains the edge (u,v) from $\mathbf{G}$ if and only if $a_{uj}\cdot a_{vj}>0$. In the fragmented graph we consider the number of connected components not counting those consisting of isolated vertices with coefficients equal to zero. We call these connected components *fragments* (of the jth fragmented graph).

In the further discussion, besides the AME method we also present drawings of fragmented graphs by using the so-called spring embedder (SE) method[18] implemented in the Vega system for manipulating discrete mathematical

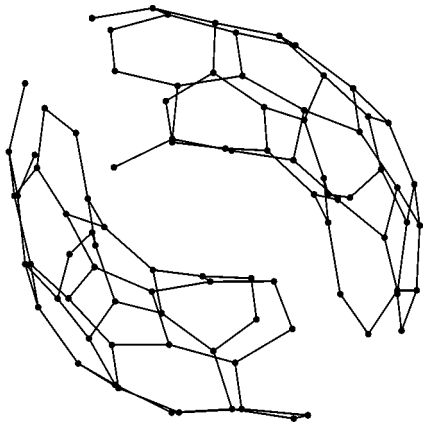

FIG. 2. A drawing (produced by the spring embedder method) of two radial-nodal fragments for the second adjacency-matrix eigenvector of the 5-6-7-ring torusene T_1, with six 5- and six 7-membered rings, having 90 vertices, is shown.

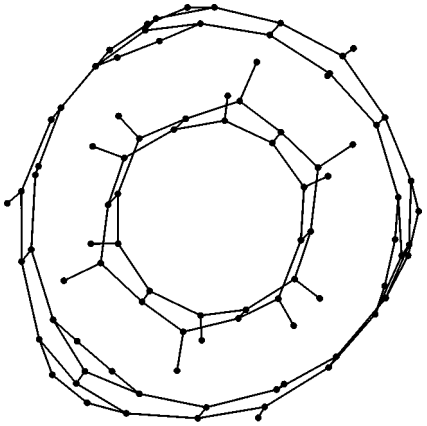

FIG. 4. The two axial-cut fragments of the 5-,6-,7-ring torusene T_1 with six 5- and six 7-membered rings having 90 vertices. The drawing was produced using the spring embedder method, and fragments are produced by the fourth eigenvector of the adjacency matrix of the torusene.

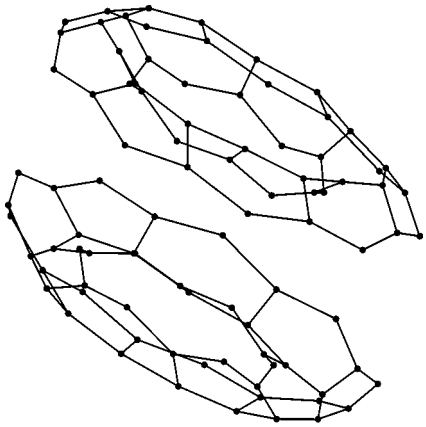

FIG. 5. The two axial-cut fragments of the 5-,6-,7-ring torusene T_1 with six 5- and six 7-membered rings having 90 vertices. The drawing was produced using the spring embedder method. Fragments are produced by the fifth eigenvector of the adjacency matrix of the torusene.

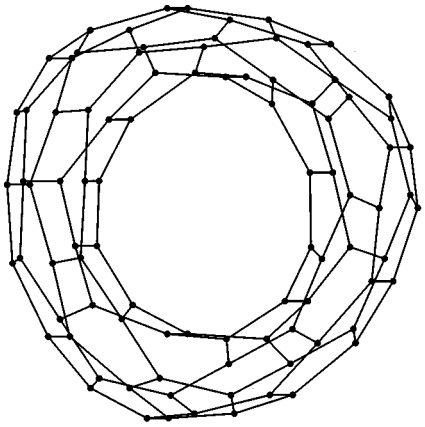

FIG. 7. A 3D-AME drawing of the torusene T_1 with 90 atoms generated by the coordinates of the triplet $\mathbf{a}_2$, $\mathbf{a}_3$, and $\mathbf{a}_5$ of the eigenvectors of the adjacency matrix of T_1.

structures.[19,20] In order to emphasize pictorially the breaking of a fragmented graph into fragments, the fragments have been separated manually.

IV. RESULTS

Now we are ready to present results, i.e., the nodal properties of the eigenvectors of selected torusenes, and to check their use in reconstructing the geometry of torusenes. In Figs. 2–5 fragmented graphs obtained from the second, third, fourth and fifth eigenvectors of 5,6,7-ring torusene T_1 with 90 vertices, six 5-rings and six 7-rings are shown.

The eigenvectors $\mathbf{a}_2$ and $\mathbf{a}_3$ correspond to degenerate free-electron wave functions with $m=0$ and $M=\pm 1$ (no axial and one radial plane), i.e., they induce two radial nodal fragments which are clearly seen in Figs. 2 and 3. The eigenvectors $\mathbf{a}_4$ and $\mathbf{a}_5$ correspond to wave functions with $m=\pm 1$ and $M=0$, i.e., they induce two axial-cut fragments which are clearly seen in Figs. 4 and 5. Note that these are topologically equivalent and one of the figures could be transformed to the other by skewing the torusene around its smaller radius.

By having at our disposal the above eigenvectors $\mathbf{a}_2$, $\mathbf{a}_3$, $\mathbf{a}_4$, and $\mathbf{a}_5$, we are now ready to check which triplet does the better job in reproducing the geometry of the torusene considered. The 3D drawing generated by the coordinates of the triplet $\mathbf{a}_2$, $\mathbf{a}_3$, and $\mathbf{a}_4$ is depicted in Fig. 6, but it is unable to reproduce the torusene as the pairs of equivalent vertices (due to the symmetry of the torus) are superimposed upon each other. However, the 3D drawing generated by the triplet $\mathbf{a}_2$, $\mathbf{a}_3$, and $\mathbf{a}_5$ shown in Fig. 7, reproduces well the geometry of torusene T_1.

In contrast, for the case of a 5,6,7-ring torusene on 120 vertices (having eight 5- and 7-membered rings) such a flexibility in choice of triplets is lost, as the fifth eigenvector generates four fragments, and the plausible geometry of this torusene is reproduced by the triplet $\mathbf{a}_2$, $\mathbf{a}_3$, and $\mathbf{a}_6$. Namely, the sixth eigenvector possess two axial-cut fragments and is a good candidate for drawing the torusene.

For all the torusenes studied here the second and third eigenvectors generate two fragments separated by a radial nodal plane. The fourth eigenvector generates an axial cut for all the torusenes studied up to one with 150 vertices. For this torusene the last term in the triplet of eigenvectors able to

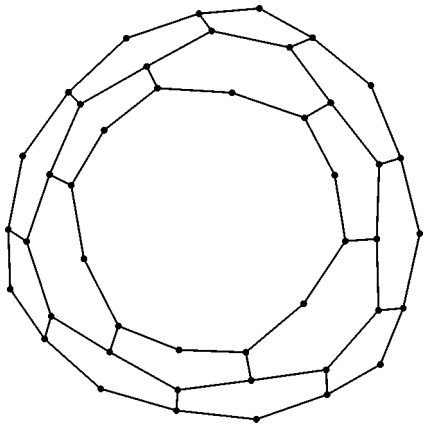

FIG. 6. A 3D-AME drawing of the torusene T_1 with 90 atoms generated by the coordinates of the triplet $\mathbf{a}_2$, $\mathbf{a}_3$, and $\mathbf{a}_4$ of the eigenvectors of the adjacency matrix of T_1.

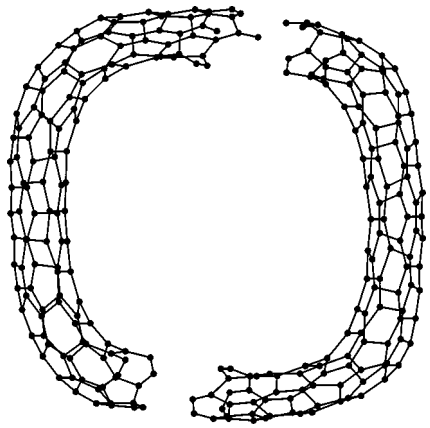

FIG. 8. Two nodal plane fragments of torusene T_2 with 270 atoms, produced by the spring embedder method, are shown for the second eigenvector of the adjacency matrix of T_2.

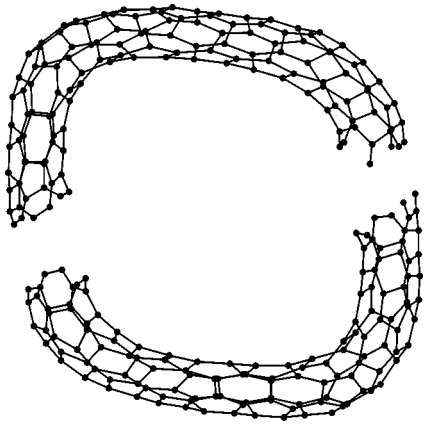

FIG. 9. Two nodal plane fragments of torusene T_2 with 270 atoms, produced by the spring embedder method, are shown for the third eigenvector of the adjacency matrix of T_2.

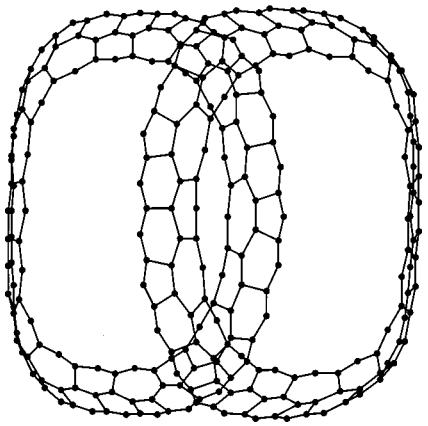

FIG. 11. Two axial-cut fragments of the torusene T_2 with 270 atoms, produced by the spring embedder method, are shown for the thirteenth eigenvector of the adjacency matrix of T_2.

reproduce a plausible geometry is either the sixth or the seventh eigenvector.

In Figs. 8–11, fragmented graphs obtained from the second, third, tenth, and thirteenth eigenvectors of the 5-,6-,7-ring torusene T_2 with 270 vertices, eighteen 5-rings and eighteen 7-rings are shown. The related AME 3D-drawings of the torusene T_2 are given in Fig. 12 for the triplet $\mathbf{a}_2, \mathbf{a}_3, \mathbf{a}_{10}$ and in Fig. 13 for the triplet $\mathbf{a}_2, \mathbf{a}_3, \mathbf{a}_{13}$. The drawing of Fig. 12 is due to the superimposition of the pairs of vertices of T_2 and is unable to reproduce the toroidal geometry, while the 3D drawing of Fig. 13 reproduces it well.

The torusenes T_1 and T_2 are the special members of the family of 5-,6-,7-ring torusenes whose building block is depicted in Fig. 14. T_1 is obtained by repetition of three, and T_2 by repetition of nine such blocks, in such a way that the final structure is closed upon itself to give a toroidal structure. The number of repeating blocks is denoted by t, and it is clear that the torusenes considered in Table I have $2t$ 5- and $2t$ 7-membered rings. Table I lists the first thirteen eigenvalues of the adjacency matrix and the corresponding number of fragments generated by the related eigenvectors as well as the quantum numbers M (of radial nodal planes) and m (of axial cuts) of the related free-electron wave functions.

Let us note that hexagonal torusenes have nearly all their eigenvalues in pairs, and some pairing is evident in 5-,6-,7-ring torusenes. Where eigenvalues occur in multiples, the exact ordering of eigenvectors is arbitrary, but this does not matter, since the final choice is made on the basis of the eigenvector's nodal properties.

V. DISCUSSION

Our numerical experiments suggest that in order to produce a plausible 3D geometry of torusenes, the second and the third eigenvectors $\mathbf{a}_2$ and $\mathbf{a}_3$ of the adjacency matrix have to be included as the first two of the optimal triplet $\mathbf{a}_2, \mathbf{a}_3, \mathbf{a}_{\text{opt}}$. The inspection of Table I shows that $\mathbf{a}_2$ generates two radial-node ($M=1$, $m=0$) fragments, and the same applies to $\mathbf{a}_3$ (where the nodal plane is orthogonal to that of $\mathbf{a}_2$). The only exception is the first of the torusenes shown in Table I, which in any case is too small to be chemically interesting due to its high strain energy. The index opt of the third eigenvector $\mathbf{a}_{\text{opt}}$ of the optimal triplet, as indicated in Table I, increases linearly with the number of t repeating building blocks, i.e., more precisely by one from $t=3$ to $t=8$ with a jump of three at the transition from $t=8$ to t

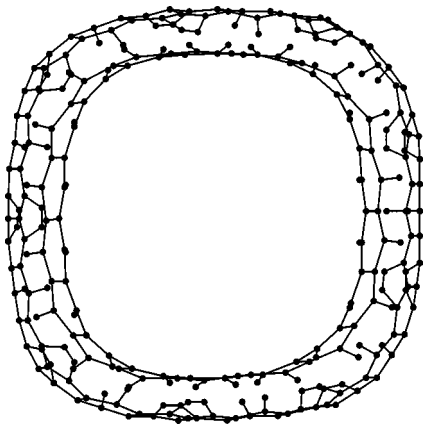

FIG. 10. Two axial-cut fragments of the torusene T_2 with 270 atoms, produced by the spring embedder method, are shown for the tenth eigenvector of the adjacency matrix of T_2.

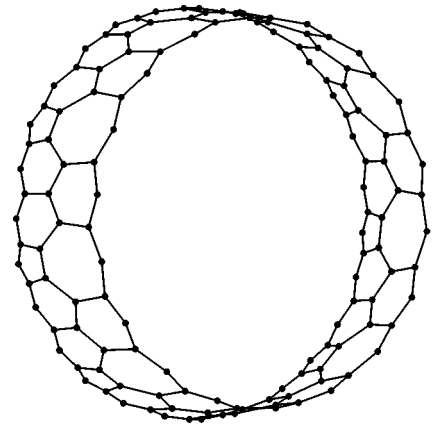

FIG. 12. A 3D-AME drawing of the torusene T_2 with 270 atoms generated by the coordinates of the triplet $\mathbf{a}_2$, $\mathbf{a}_3$, and $\mathbf{a}_{10}$ of the eigenvectors of the adjacency matrix of T_2.

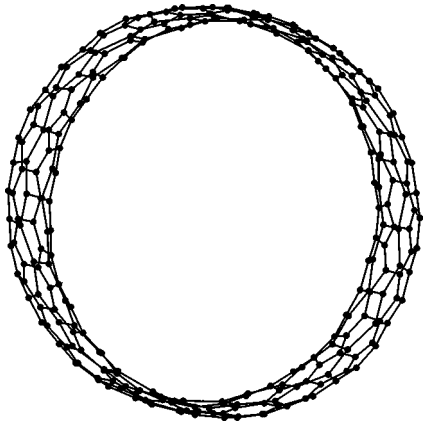

FIG. 13. A 3D-AME drawing of the torusene T_2 with 270 atoms generated by the coordinates of the triplet $\mathbf{a}_2$, $\mathbf{a}_3$, and $\mathbf{a}_{13}$ of the eigenvectors of the adjacency matrix of T_2.

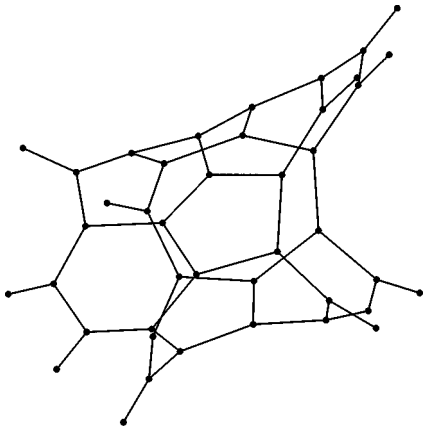

FIG. 14. The building block of the torusenes given in Table I.

$=9$. Note that every $\mathbf{a}_{\text{opt}}$ has one axial cut ($M=0$, $m=1$), which appears to be a necessary condition in order to reproduce the geometry of torusene. However, this condition is not sufficient, as can be seen from Table I. For the torusene T_1 the eigenvector $\mathbf{a}_4$ has also one axial cut, but the next one, $\mathbf{a}_5$, with the same property, is taken as the member of the optimal triplet.

These findings have their quantum mechanical explanation; namely, the ratio of large and small radii of the torusene

TABLE I. Thirteen largest eigenvalues λ_j, numbers of fragments #fr for corresponding adjacency matrix eigenvectors and the related quantum numbers M and m for selected torusenes on n vertices built up by repetition of t building blocks of Fig. 14, and counting $2t$ 5- and $2t$ 7-membered rings. The asterisk by some #fr entries indicates a situation discussed in the text. The choice of the third element of the optimal triplet of eigenvectors $\mathbf{a}_2, \mathbf{a}_3, \mathbf{a}_{\text{opt}}$ as discussed in the text is denoted by underlining the corresponding #fr.

	Example T_1															
	$n=60$, $t=2$				$n=90$, $t=3$				$n=120$, $t=4$				$n=150$, $t=5$			
j	λ_j	#fr	M	m	λ_j	#fr	M	m	λ_j	#fr	M	m	λ_j	#fr	M	m
1	3	1	0	0	3	1	0	0	3	1	0	0	3	1	0	0
2	2.6681	2	0	1	2.8301	2	1	0	2.9015	2	1	0	2.9360	2	1	0
3	2.6645	2	1	0	2.8301	2	1	0	2.9015	2	1	0	2.9360	2	1	0
4	2.6458	2	0	1	2.6681	2	0	1	2.6681	2	0	1	2.7624	4	2	0
5	2.6209	2	1	0	2.6458	2	0	1	2.6645	4	2	0	2.7624	4	2	0
6	2.3018	4	1	1	2.4822	3*	1	1	2.6458	2	0	1	2.6681	2	0	1
7	2.2775	4	1	1	2.4822	3*	1	1	2.6209	4	2	0	2.6458	2	0	1
8	2.2160	4	1	1	2.4814	4	1	1	2.5569	4	1	1	2.5966	3*	1	1
9	2.1909	4	1	1	2.4814	4	1	1	2.5569	4	1	1	2.5966	3*	1	1
10	1.8712	5*	2	1	2.3822	3*	2	0	2.5520	4	1	1	2.5853	4	1	1
11	1.8224	4	0	2	2.3822	3*	2	0	2.5520	4	1	1	2.5853	4	1	1
12	1.7840	4	2	0	2.0498	8	2	1	2.3018	4	2	1	2.5126	6	3	0
13	1.7321	4	0	2	2.0498	8	2	1	2.2775	4	2	1	2.5126	5*	3	0
	Example T_2															
	$n=180$, $t=6$				$n=210$, $t=7$				$n=240$, $t=8$				$n=270$, $t=9$			
j	λ_j	#fr	M	m	λ_j	#fr	M	m	λ_j	#fr	M	m	λ_j	#fr	M	m
1	3	1	0	0	3	1	0	0	3	1	0	0	3	1	0	0
2	2.9552	2	1	0	2.9669	2	1	0	2.9746	2	1	0	2.9799	2	1	0
3	2.9552	2	1	0	2.9669	2	1	0	2.9746	2	1	0	2.9799	2	1	0
4	2.8301	4	2	0	2.8729	4	2	0	2.9015	4	2	0	2.9215	4	2	0
5	2.8301	4	2	0	2.8729	4	2	0	2.9015	4	2	0	2.9215	4	2	0
6	2.6681	2	0	1	2.7312	6	3	0	2.7888	6	3	0	2.8301	6	3	0
7	2.6645	6	3	0	2.7312	6	3	0	2.7888	6	3	0	2.8301	6	3	0
8	2.6458	2	0	1	2.6681	2	0	1	2.6681	2	0	1	2.7135	8	4	0
9	2.6209	6	3	0	2.6458	2	0	1	2.6645	8	4	0	2.7135	8	4	0
10	2.6184	4	1	1	2.6316	3*	1	1	2.6458	2	0	1	2.6681	2	0	1
11	2.6184	2*	1	1	2.6316	3*	1	1	2.6401	2*	1	1	2.6460	3*	1	1
12	2.6037	4	1	1	2.6148	4	1	1	2.6401	2*	1	1	2.6460	3*	1	1
13	2.6037	4	1	1	2.6148	4	1	1	2.6220	4	1	1	2.6458	2	0	1

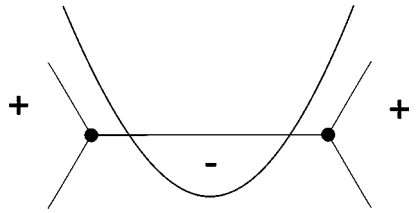

FIG. 15. The case, discussed in the text, when two nodal surfaces pass through a single edge.

$q=R/r$ is proportional to t and as it increases, the torusene starts to resemble the circumference, whose free-electron wave functions are described basically by $\sin M\Phi$ or $\cos M\Phi$ with axial cut wave functions appearing at the very high energies, i.e., at a high order of $\mathbf{a}_{\mathrm{opt}}$. Recall that due to the negative value of the interaction between adjacent atoms, the ordering of the adjacency-matrix eigenvalues is exactly opposite to the orderings of energies of electrons in the molecule described conventionally by a graph.

Although the parallelism between the eigenvectors and the free electron wave functions has appeared to be fruitful, one should be aware of the situation depicted in Fig. 15, where it is shown that two nodal surfaces passing through an edge will not be recognized as leading to two different fragments of a graph. This means that the number of fragments as generated by the eigenvectors is smaller or equal to the number induced by wave functions (which is always even and given by $2M\times 2m$). An example is offered by #fr=3* of the torusene T_1, where four fragments $(2M\times 2m=4)$ have merged to three due to the discrete nature of the vertices being embedded onto the continuous surface of the torus.

Finally, note that if one cuts a torus, keeps one end fixed, and rotates the other by multiples of 2π, before regluing (identifying) the ends, a series of twisted tori is obtained (in principle, although clearly not in practice, an infinite number). Note, however, that ''twist'' is relative, and which one is ''untwisted'' may just be a matter of convention. In any case, all of them exhibit the same connectivity.[11,21] The construction used to identify many different toroidal tilings with a common graph[21] can be modified to yield a unique label, which in extended form also labels the topologically distinct embeddings, and is also treated in Ref. 22. A question then arises as to which one of these isomorphic tori will be reproduced by the triplet of selected eigenvectors. Our experiments so far suggest that as a rule untwisted tori are reproduced (the ones we guess to have the lowest quantum-mechanical energy), although a few twisted ones have been observed, as indicated by appropriate twisting of the respective axial cuts. It is possible that a more exhaustive search among the eigenvectors might in some cases reveal more than one plausible drawing, each modelling a differing degree of twist.

VI. CONCLUSIONS

The problem of choice of the optimal triplet of eigenvectors, $\mathbf{a}_j,\mathbf{a}_k,\mathbf{a}_l$, being able to reproduce (within the AME method) plausible geometries of torusenes has been addressed in this paper. Theoretical and computer experimental considerations presented here suggest that the triplet $\mathbf{a}_2,\mathbf{a}_3,\mathbf{a}_{\mathrm{opt}}$ fulfills the task where the $\mathbf{a}_{\mathrm{opt}}$ should be searched for among those eigenvectors which possess no nodal plane but one axial cut. In the present paper these findings have been elaborated for 5-,6-,7-ring torusenes with up to 270 atoms, but computer experiments have shown that similar findings hold for purely polyhex torusenes with up to 224 carbon atoms as well.

ACKNOWLEDGMENTS

This work was supported by the Ministry of Science and Technology of Slovenia (Grants Nos. I1-616-0101-97 and I2-6193-0101-97), Ministry for Science of Croatia (Grant No. 0090606), and the Slovenian–Croatian joint project Discrete mathematics in Chemistry.

[1] H. W. Kroto, W. Allaf, and S. P. Bahn, Chem. Rev. **91**, 1213 (1991).
[2] W. P. Thurston, Research Report No. GCG 7, Geometry Center, University of Minnesota.
[3] G. Brinkman and A. W. M. Dress, Proc. Acad. Sci. Am., J. Algorithms **23**, 345 (1997).
[4] H. W. Kroto, Nature (London) **329**, 529 (1987).
[5] T. G. Schmalz, W. A. Seitz, D. J. Klein, and G. E. Hite, J. Am. Chem. Soc. **110**, 1113 (1988).
[6] D. E. Manolopoulos and P. W. Fowler, J. Chem. Phys. **96**, 7603 (1992).
[7] J. Shawe-Taylor and T. Pisanski, Technical Report No. CSD-TR-93-20, Royal Holloway, University of London, Department of Computer Science, Egham, Surrey TW20 OEX, England (in press).
[8] P. W. Fowler, T. Pisanski, and J. Shawe-Taylor, in *Graph Drawing*, edited by R. Tamassia and I. G. Tollis, Lecture Notes in Computer Science (Springer, Berlin, 1995), pp. 894, 282.
[9] T. Pisanski, B. Plestenjak, and A. Graovac, Croat. Chem. Acta **68**, 283 (1995).
[10] J. Liu, H. J. Dai, J. H. Hafner, D. T. Colbert, R. E. Smalley, S. J. Tans, and C. Dekker, Nature (London) **385**, 780 (1997).
[11] E. C. Kirby, *From Chemical Topology to Three-Dimensional Geometry*, edited by A. T. Balaban (Plenum, New York, 1997), pp. 263–296, and references therein.
[12] Y. Jiang, Y. Shao, and E. C. Kirby, Fullerene Sci. Technol. **2**, 481 (1994).
[13] E. C. Kirby and T. Pisanski, J. Math. Chem. **23**, 151 (1998).
[14] D. J. Klein and H. Zhu, Discrete Appl. Math. **67**, 157 (1996).
[15] E. C. Kirby and P. Pollack, J. Chem. Inf. Comput. Sci. **38**, 66 (1998); **38**, 1256 (1998).
[16] P. E. John, Croat. Chem. Acta **71**, 435 (1998).
[17] J. Friedman, Duke Math. J. **69**, 487 (1993).
[18] T. Fruchtermann and E. Reingold, Software-Practice and Experience **21**, 1120 (1991).
[19] T. Pisanski, Vega Version 0.2 Quick Reference Manual and Vega Graph Gallery, Commission for the DMFA publications, Jadranska 19, SI-1111 Ljubljana, Slovenia, 1995.
[20] T. Pisanski *et al.*, ''Vega: System for manipulating discrete mathematical structures,'' Available on http://vega.ijp.si/.
[21] D. J. Klein, J. Chem. Inf. Comp. Sci. **34**, 453 (1998).
[22] J. Szucz and D. J. Klein, Discr. Math. (to be published).